PROCEEDINGS of the
23rd International Congress on Acoustics

9 to 13 September 2019 in Aachen, Germany

Dispersion-reduced time domain FEM for room acoustics simulation

Takeshi OKUZONO(1), Kimihiro SAKAGAMI(2), Toru OTSURU(3)

(1)Kobe University, Japan, okuzono@port.kobe-u.ac.jp
(2)Kobe University, Japan, saka@kobe-u.ac.jp
(3)Oita University, Japan, otsuru@oita-u.ac.jp

Abstract

This paper presents an overview of the applicability of implicit time-domain FEM (TD-FEM) for room acoustics simulation, which has fourth-order accuracy in both space and time. First, the TD-FEM algorithm is presented with explanations of dispersion-reduced finite elements for spatial discretization and a time integration method for time discretization. The theoretical dispersion error property is also shown. Use of the dispersion-reduced scheme presents benefits in terms of accuracy, stability and convergence of an iterative solver, which have a marked effect on the computational cost. Then, the applicability of TD-FEM is demonstrated using two numerical examples on room acoustics simulation in the kilohertz frequency range, which are acoustics simulations of a simply shaped concert hall and simulation of reverberation absorption coefficient measurements. In numerical examples of concert hall analysis, comparison with a conventional TD-FEM presents the efficiency of the dispersion-reduced TD-FEM. Modeling accuracy of non-locally reacting permeable membrane sound absorbers for the TD-FEM is presented through simulation of reverberation room method.

Keywords: Finite element method, Room acoustics simulation, Wave acoustics

1 INTRODUCTION

Wave-based room acoustic simulations, which solve a wave equation numerically under appropriate boundary conditions, can accurately simulate sound propagation inside rooms. Nevertheless, they entail an important shortcoming: computationally, they are too expensive because of the large dimensions of the architectural space. Therefore, discretization of a wave equation accurately using less computational resources is a primary concern for practical applications. Recently, direct time domain simulations have garnered considerable attention. Various efficient time domain wave-based solvers have been proposed, with numerous unique benefits and shortcomings [1, 2, 3, 4, 5, 6, 7, 8]. Actually, time-domain finite element method (TD-FEM) is an attractive solver, especially for complex shaped room acoustics simulation, with the inherent capability of modeling complex geometries by finite element discretization of space. The algorithm can be made unconditionally stable simply by changing a parameter for the standard formulation. Derivation of the stability condition is simple, even in simulations of complex-shaped rooms using conditionally stable algorithms. These features are also favorable for room acoustics simulation. However, the algorithm is generally implicit, with complex implementation because of the requirement of matrix operation. Combined usage of sparse matrix storage formats and iterative solvers is quite important for large-scale analyses. In addition, inherent space and time discretization errors called dispersion errors must be reduced to conduct large-scale room acoustics simulations efficiently.

Recently, the authors have undertaken development of dispersion-reduced TD-FEM using low-order FEs for large-scale room acoustics simulations. It has fourth-order accuracy in both space and time for an idealized condition. This paper presents an overview of the our recent developments [4, 9], with demonstrations of its applicability to large-scale room acoustics simulation. For the demonstrations, the accuracy and efficiency over a conventional second-order accurate TD-FEM are first presented by the simulation of a simply shaped concert hall. The validity is further demonstrated by the direct simulation of reverberation absorption coefficient measurement for single-leaf permeable membrane sound absorbers. The paper contents are based on our earlier work [4, 9], but explanations of the development on a higher-order spline method can be found in other reports of the relevant literature [1, 3, 7].

2 DISPERSION REDUCED TIME DOMAIN FEM [4]

2.1 Space and time discretization of the wave equation

We consider sound propagation in a closed sound field governed by a nonhomogeneous wave equation expressed with sound pressure p as

$$\frac{\partial^2 p}{\partial^2 t} - c_0^2 \nabla^2 p = \rho_0 c_0^2 \frac{\partial q}{\partial t}, \tag{1}$$

where ρ_0 signifies the air density, c_0 stands for the speed of sound in air, and q denotes the added fluid mass per unit volume. The air domain is spatially discretized using linear hexahedral FEs with a dispersion reduction method called modified integration rules (MIR) [10]. Use of MIR has three appealing characteristics: reduction of dispersion error, relaxation of the stability condition, and accelerating convergence of the iterative solver. Those characteristics are demonstrated later through numerical examples. Introducing FE discretization to the weak form of nonhomogeneous wave equation and inserting boundary conditions give the following semi-discretized matrix equation as

$$\mathbf{M}\ddot{\mathbf{p}} + c_0^2 \mathbf{K}\mathbf{p} + c_0 \mathbf{C}\dot{\mathbf{p}} = \mathbf{f}, \tag{2}$$

Here, $\mathbf{M}$, $\mathbf{K}$, and $\mathbf{C}$ respectively represent the global mass matrix, global stiffness matrix, and global dissipation matrix in terms of the air domain. The two vectors $\mathbf{p}$ and $\mathbf{f}$ respectively represent sound pressure at all nodes and the external force. Further applying a direct time integration method called Newmark β method in the temporal direction, which can control stability by a parameter β, yields the following time-marching scheme.

$$[\mathbf{M} + \beta \Delta t^2 c_0^2 \mathbf{K} + 0.5 c_0 \Delta t \mathbf{C}]\ddot{\mathbf{p}}^{n+1} = \mathbf{f}^{n+1} - c_0 \mathbf{C}\mathbf{P} - c_0^2 \mathbf{K}\mathbf{Q}, \tag{3}$$

$$\mathbf{p}^{n+1} = \mathbf{p}^n + \Delta t \dot{\mathbf{p}}^n + \Delta t^2 (0.5 - \beta)\ddot{\mathbf{p}}^n + \Delta t^2 \beta \ddot{\mathbf{p}}^{n+1}, \tag{4}$$

$$\dot{\mathbf{p}}^{n+1} = \dot{\mathbf{p}}^n + 0.5 \Delta t (\ddot{\mathbf{p}}^n + \ddot{\mathbf{p}}^{n+1}), \tag{5}$$

with

$$\mathbf{P} = \dot{\mathbf{p}}^n + 0.5 \Delta t \ddot{\mathbf{p}}^n, \quad \mathbf{Q} = \mathbf{p}^n + \Delta t \dot{\mathbf{p}}^n + \Delta t^2 (0.5 - \beta)\ddot{\mathbf{p}}^n. \tag{6}$$

Here, Δt represents the time interval. The linear system of Eq. (3) is solvable efficiently using a preconditioned iterative solver, Conjugate Gradient (CG) method, with diagonal scaling. The present paper uses the highly accurate Fox–Goodwin (FG) method, which is known as a Newmark method with $\beta = 1/12$. Regarding the data structure of storing matrix components of Eq. (3), sparse storage formats such as the compressed row storage format, which do not store zero elements, provide the benefit of reducing or limiting the memory requirements because the matrices of Eq. (3) are sparse and include many zero elements.

2.2 Modified integration rules and 3D dispersion relations

MIR [10] is Gauss–Legendre rule with modified integration points to calculate the element stiffness matrix $\mathbf{k_e}$ and mass matrix $\mathbf{m_e}$. It requires no additional computational cost. For linear hexahedral FEs, Gauss–Legendre rules in three dimensions are defined as

$$\mathbf{k_e} \simeq \sum_{i=1}^{8} w_i \nabla \mathbf{N}(\alpha_{k,i}, \alpha_{k,i}, \alpha_{k,i})^{\mathrm{T}} \nabla \mathbf{N}(\alpha_{k,i}, \alpha_{k,i}, \alpha_{k,i}) \det(\mathbf{J}), \tag{7}$$

$$\mathbf{m_e} \simeq \sum_{i=1}^{8} w_i \mathbf{N}(\alpha_{m,i}, \alpha_{m,i}, \alpha_{m,i})^{\mathrm{T}} \mathbf{N}(\alpha_{m,i}, \alpha_{m,i}, \alpha_{m,i}) \det(\mathbf{J}), \tag{8}$$

where $\alpha_{k,i}$ and $\alpha_{m,i}$ are coordinates of the i-th integration point for $\mathbf{k_e}$ and $\mathbf{m_e}$, w_i is the weight of i-th integration points, $\mathbf{J}$ is the Jacobian matrix. For the conventional Gauss quadrature rule, $\alpha_{k,i} = \alpha_{m,i} = \pm 1/\sqrt{3}$ and

$w_i = 1$. Instead of the conventional points, MIR use modified integration points, which are derived from theoretical dispersion error analyses for an idealized condition, and which are given for the Fox–Goodwin method as

$$\alpha_{k,i} = \alpha_{m,i} = \pm\sqrt{2/3}. \tag{9}$$

The points above inherently eliminate a second-order error term attributable to spatial discretization. It can be shown that the dispersion-reduced TD-FEM has fourth-order accuracy in terms of dispersion error via theoretical dispersion error analysis. In the theoretical analysis, an ideal plane wave propagation in a free field is assumed under a spherical coordinate system with uniformly discretized rectangular grid. The theoretically estimated dispersion error $e_{\text{dis.}}$ is given as [4]

$$e_{\text{dis.}} \simeq \frac{k^4}{480}[d_x^4\cos^6\phi\sin^6\theta + d_y^4\sin^6\phi\sin^6\theta + d_z^4\cos^6\theta - c^4\Delta t^4]. \tag{10}$$

Therein, k, θ, and ϕ respectively denote the wavenumber, azimuth, and elevation. The element sizes of rectangular FEs in the x, y, and z directions are denoted respectively by d_x, d_y, and d_z. For the TD-FEM using conventional Gauss rule the order of dispersion error is of second order as presented below

$$e_{\text{dis.}} \simeq \frac{k^2}{24}[d_x^2\cos^4\phi\sin^4\theta + d_y^2\sin^4\phi\sin^4\theta + d_z^2\cos^4\theta]. \tag{11}$$

Equation (11) includes only spatial discretization error, indicating that FG method is inherently fourth-order accurate. The sound speed in dispersion-reduced TD-FEM becomes slower when using coarser mesh, whereas the sound speed increases in the conventional TD-FEM.

2.3 Stability condition

The dispersion-reduced TD-FEM using FG method is conditionally stable, but the stability limit is more relaxed than the conventional TD-FEM. The stability condition for arbitrary element shape is given as

$$\Delta t \leq \frac{1}{\omega_{\max}\sqrt{1/4-\beta}}. \tag{12}$$

In that expression, $\omega_{\max}$ is the maximum natural frequency calculated from a generalized eigenvalue problem $(\mathbf{k_e} - k^2\mathbf{m_e})\mathbf{p_e} = 0$ for all elements. The solution of the eigenvalue problem is trivial because it is the element level calculation. For rectangular FEs, Eq. (12) can be written simply as [4]

$$\Delta t \leq \frac{1}{c\sqrt{\frac{1}{d_x^2}+\frac{1}{d_y^2}+\frac{1}{d_z^2}}}. \tag{13}$$

The dispersion reduced TD-FEM can use a $\sqrt{2}$ times larger time interval than the stability condition of conventional TD-FEM, which is given below:

$$\Delta t \leq \frac{1}{\sqrt{2}c\sqrt{\frac{1}{d_x^2}+\frac{1}{d_y^2}+\frac{1}{d_z^2}}}. \tag{14}$$

3 APPLICATIONS

3.1 Simply shaped concert hall

The efficiency of the dispersion-reduced TD-FEM is presented in a comparison with the conventional second-order accurate TD-FEM through the acoustics simulation of a simply shaped concert hall with volume of 8,056

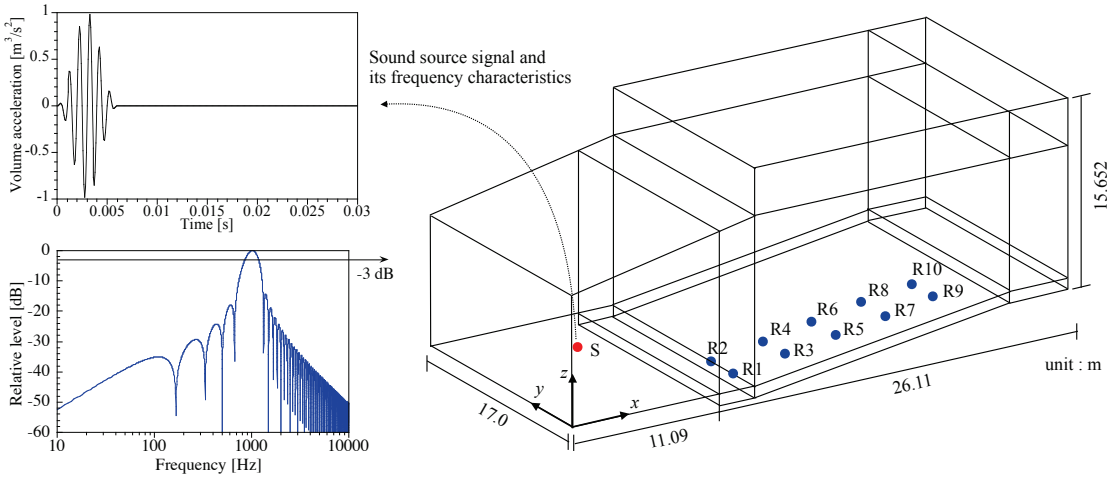

Figure 1. A CAD model of a hall with a source and ten receiving points.

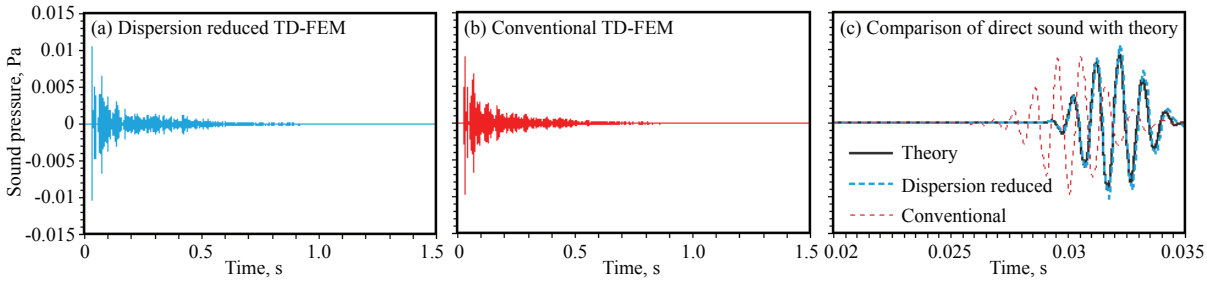

Figure 2. Waveforms at R1 calculated using (a) dispersion-reduced TD-FEM, (b) conventional TD-FEM, and (c) comparison of direct sound at R1 with theory.

m^3. Figure 1 presents the analyzed hall which has 49,172,384 degrees of freedom. The mesh satisfies a spatial resolution of 4.3 elements per wavelength at the upper-limit frequency of 1.4 kHz. The spatial resolution is much smaller than the well known rule of thumb for linear elements, i.e., ten elements per wavelength. Therefore, the sound speed in the conventional method becomes greater than the exact value of c_0. A point source S is placed at the center of stage (1.2 m height). A tone-burst signal with six waves of 1 kHz center frequency is used as the sound source signal. The band-limited impulse response is calculated up to 1.6 s at 10 receivers R1∼R10. The equivalent impedance model [3] is used to model sound absorption at the boundary surfaces. The averaged sound absorption coefficient in the hall is 0.27. Time intervals used for the dispersion-reduced TD-FEM and conventional TD-FEM are, respectively, Δt=1/12,000 s and Δt=1/17,000 s. The respective stability limits for both methods are 1/11,702 s and 1/16,549 s. Here, the dispersion reduced method can reduce the total time steps of analyses to $1/\sqrt{2}$ of those used for the conventional method.

Figures 2(a)–2(c) respectively show overall impulse responses at R1 for both methods and a comparison of direct sound at R1 with theoretical values. Dispersion-reduced TD-FEM shows good agreement with theory, but the arrival time of direct sound in the conventional method is earlier than that of theory. Figure 3 portrays sound pressure distributions at 30 ms and 80 ms for both dispersion-reduced TD-FEM and conventional TD-FEM. Dispersion-reduced TD-FEM shows isotropic sound propagations with smaller dispersion error, but the conventional TD-FEM shows anisotropic propagations because of its larger dispersion error. The conventional

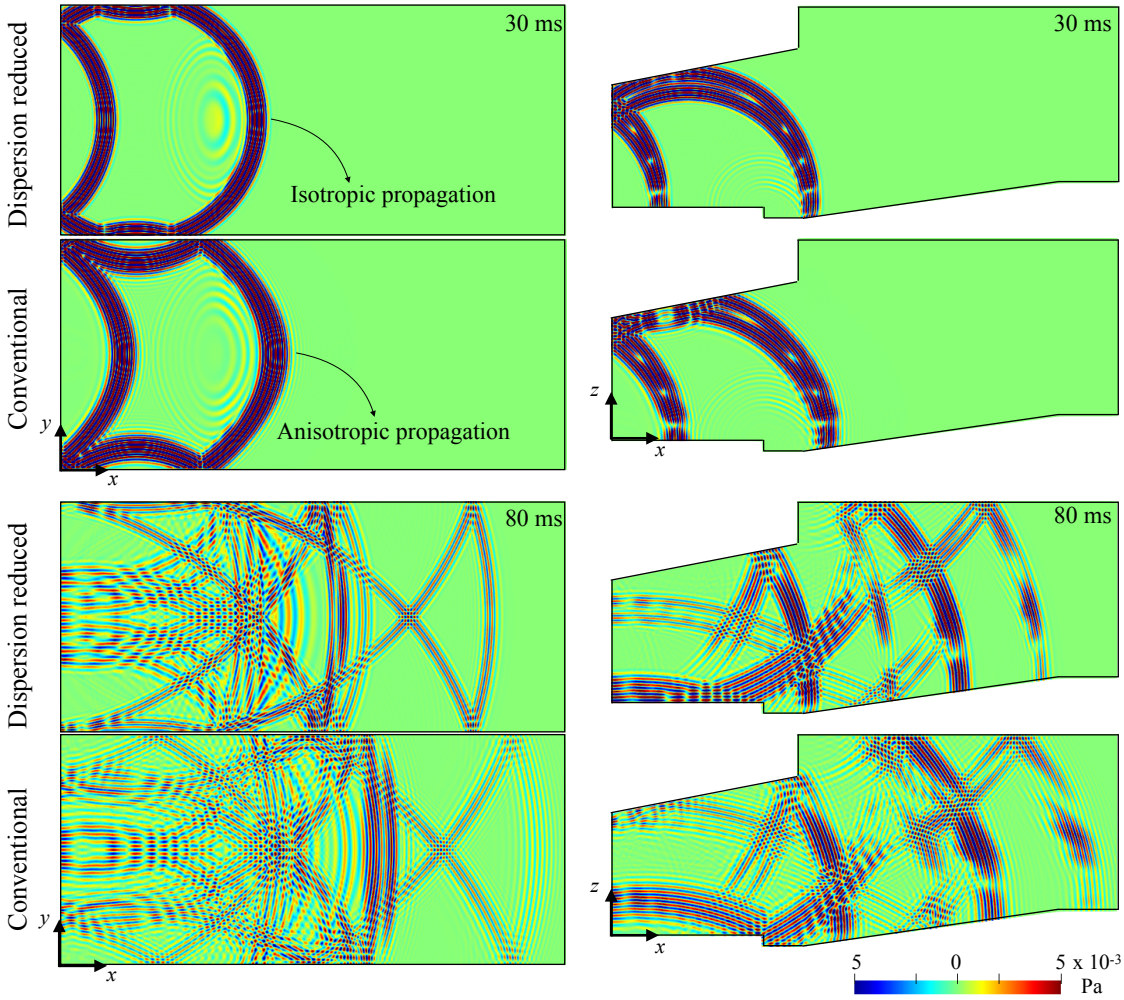

Figure 3. Sound pressure distributions in the hall calculated using dispersion-reduced TD-FEM and conventional TD-FEM: xy–plane at z=2.7 m (left) and zx–plane at y=8.5 m (right).

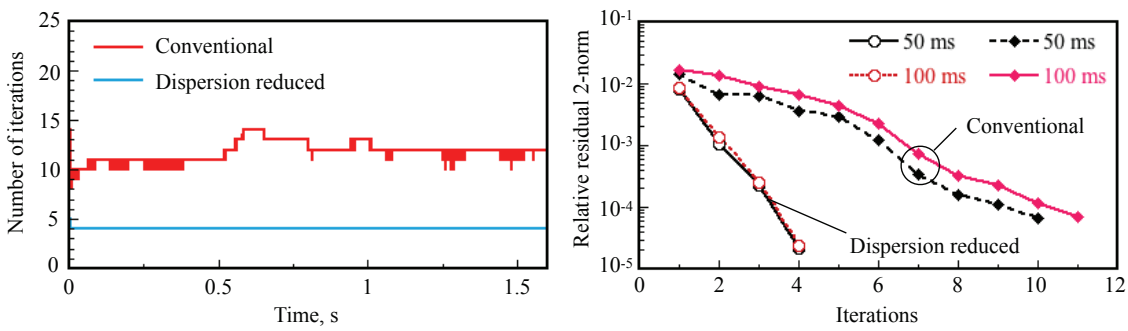

Figure 4. Iteration numbers of CG method at each time step (left), and convergence history of CG method at time t = 50 ms and 100 ms (right). The convergence tolerance is set to 10^{-4}.

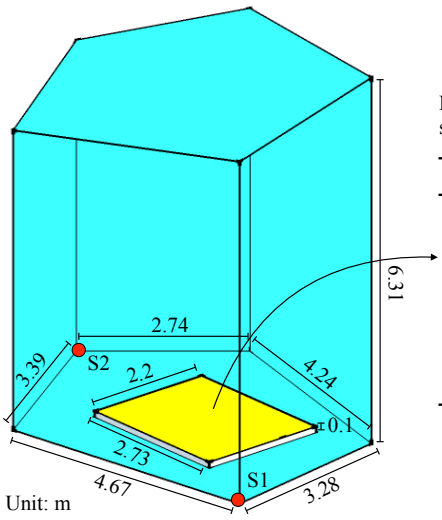

Material parameters of eight PMs #1-#8: flow resistance R, surface density M, and thickness t

Permeable membrane	R, Pa s/m	M, kg/m^2	t, mm
#1 PET cloth A	196 ($0.47\rho_0c_0$)	0.06	0.16
#2 PET cloth B	462 ($1.12\rho_0c_0$)	0.12	0.20
#3 Glass fiber cloth	1200 ($2.90\rho_0c_0$)	0.21	0.18
#4 PET high-density woven fabric	1050 ($2.54\rho_0c_0$)	0.20	0.48
#5 PP non-woven fabric A	64 ($0.15\rho_0c_0$)	0.13	0.39
#6 PP non-woven fabric B	221 ($0.53\rho_0c_0$)	0.24	0.59
#7 PET non-woven fabric A	70 ($0.17\rho_0c_0$)	0.08	0.31
#8 PET non-woven fabric B	80 ($0.19\rho_0c_0$)	0.08	0.31

Single-leaf PM absorber has a backing air cavity of 0.1 m in depth

Figure 5. Numerical reverberation chamber model including a single-leaf PM absorber and material property of eight permeable membranes. [9]

method has larger dispersion error for axial directions than oblique directions. Therefore, the sound speed in axial directions becomes faster than that in oblique directions, as might be apparent in Figure 3. Figure 4 presents the iteration numbers of CG method at each time step for both the methods and the convergence history at 50 ms and 100 ms. The iteration number corresponds to the number of matrix-vector products, which comprise a large percentage of operations in TD-FEM. It is particularly interesting that the dispersion-reduced TD-FEM has better matrix property for the convergence of iterative solver, showing a rapid residual reduction. The mean iteration number per time step is 4, whereas the number is 11.8 for the conventional method. Therefore, the computational complexity of dispersion reduced method is reduced to 1/3 of that of conventional method with the same mesh, including the effect of time step reduction. These effects are notable benefits of the dispersion-reduced method as well as the effect of reducing the dispersion error.

3.2 Reverberation absorption coefficient measurements

Permeable membranes (PMs), which are air-permeable thin woven fabrics or non-woven fabrics, are attractive sound-absorbing materials. Various PM absorbers have been proposed to date, such as acoustic curtains, suspended acoustic ceilings, and space sound absorbers [11, 12, 13]. In this section, the absorption characteristics of the most classical single-leaf PM absorber (PMSG), in which a PM is placed in front of a rigid-backed air cavity, are predicted by the simulation of reverberation absorption coefficient measurements, and are compared with measured values to demonstrate the further applicability of dispersion-reduced TDFEM. Figure 5 shows the simulated reverberation room (130 m^3 volume and 153 m^2 surface area), which includes detailed information about the installed materials. The material properties are all measured values. Eight PMs, each with different flow resistance and surface density, are used for comparison. All materials are thin woven fabrics or non-woven fabrics made of general purpose chemical fibers such as PET, PP, and glass fibers. The reverberation absorption coefficient measurements are found based on JIS A 1409 standard, except for the area of the test specimen, with an integrated impulse response method. In the simulations, calculations are done in the empty room and in the room containing the absorber to calculate the absorption coefficient at frequencies of 100 Hz to 2.5 kHz. Three frequency bands (low, medium, and high frequencies) are considered in the calculations to simulate the frequency dependence of absorption characteristics of the room's boundary surface. Here, the low-frequency band includes frequencies of 100 Hz – 500 Hz. Mid-frequency and high-frequency bands respectively include

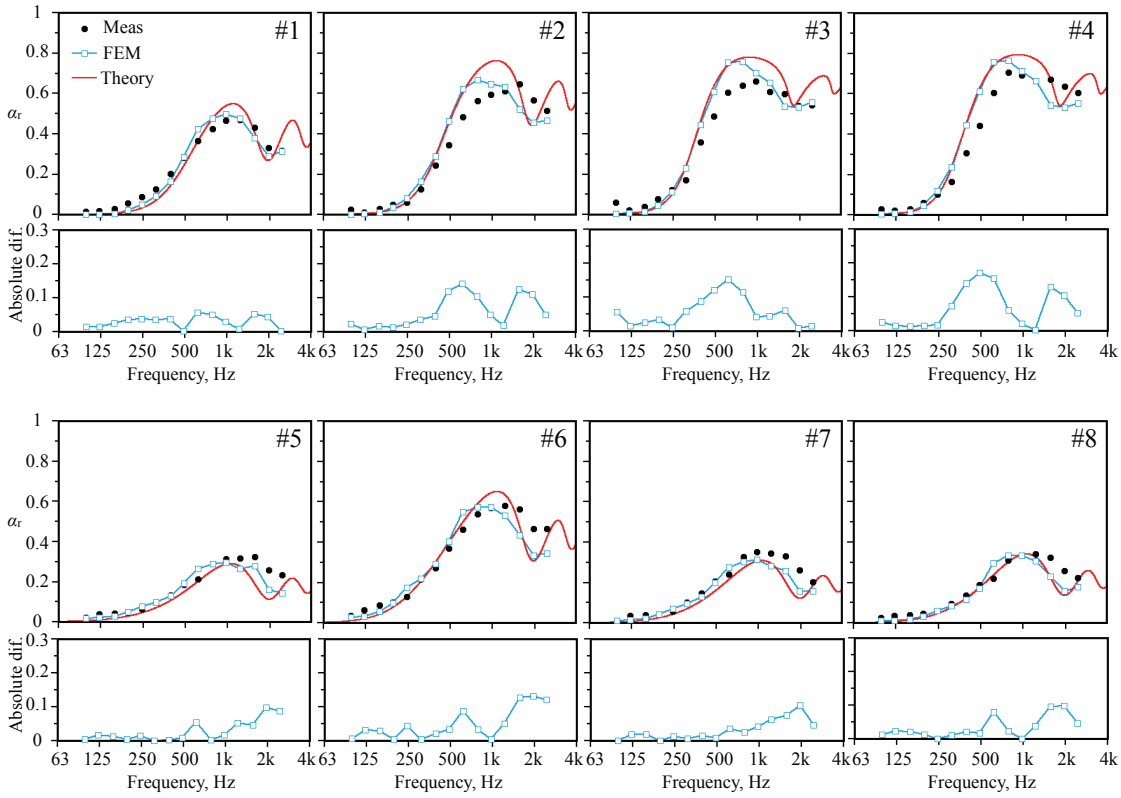

Figure 6. Comparison of reverberation absorption coefficient of PMSG using membranes of #1–#8 among measurement, theory and dispersion-reduced TD-FEM. [9]

frequencies of 630 Hz to 1.25 kHz, and of 1.6 kHz to 2.5 kHz. For the boundary surface of the room, equivalent impedance values corresponding to 0.0124, 0.0189, and 0.0275 are given respectively at low-, medium-, and high-frequency bands. Band-limited impulse responses are calculated up to 13.0 s, 9.0 s, and 5.0 s for the respective frequency bands, with a sound source signal, which is the impulse response of optimized FIR filter based on the Parks–McClellan algorithm. PMs are modeled using limp PM elements [9]. Two FE meshes with different spatial resolution are created for low and medium-frequency bands and high-frequency band, which respectively satisfy five elements per wavelength at the upper-limit frequencies of 1,414 Hz and 2,828 Hz. As a reference, the resulting total numbers of elements of finer FE mesh are 17,632,256 in the empty model, 18,608,148 in the room model containing the absorbers. The time intervals are set to 1.2195×10^{-5}s for the empty model and 1.14943×10^{-5}s for the room model containing the absorbers.

Figure 6 presents a comparison of reverberation absorption coefficients α_r of PMSG using membranes #1–#8 among measurement (Meas), FEM value and the theoretical statistical values. The absolute difference of the absorption coefficient between measurements and FEM is also shown in the figure. As a well known feature, PMSG can not offer a highly diffuse field absorption coefficient at low frequencies because of the effect of non-locally reacting rigid-backed air cavity [14]. This feature is apparent in both FEM and measured results. Overall, considering measurement uncertainty, FEM results were found to agree well with measured results. Better agreement can be found in the results of membranes #1, #5, #7, and #8, with mean absolute difference values less than 0.033. In future works, the present numerical reverberation chamber is useful for PM sound absorber designs with complex configurations. In addition, the limp PM elements are expected to be useful to model the sound absorption characteristics of acoustic curtains, suspended acoustic ceilings, and space sound

absorbers.

4 CONCLUSIONS

This paper presented an overview of the dispersion-reduced TD-FEM for room acoustics simulation and its applicability, based on our recent developments. The first numerical example clearly showed a considerable benefit of the dispersion reduction method to conduct large-scale room acoustics simulation efficiently without reducing accuracy. Then, the second numerical example demonstrated the applicability of dispersion reduced TD-FEM toward sound absorber design by numerical reverberation chamber tests. It can be concluded that the dispersion-reduced TD-FEM has promising potential to simulate acoustics of practical sized rooms at kilohertz frequencies.

ACKNOWLEDGEMENTS

This work was supported in part by JSPS KAKENHI Grant No. 17K14771. The computations were conducted mainly using computer facilities at the Research Institute for Information Technology, Kyushu University.

REFERENCES

[1] Otsuru T, et al. Applications of large-scale finite element sound field analysis onto room acoustics. Proceedings of 19th International Congress on Acoustics, Madrid, Spain, September 2–7, 2007. In CD-ROM.

[2] Sakamoto S, Nagatomo H, Ushiyama A, Tachibana H. Calculation of impulse responses and acoustic parameters in a hall by the finite-difference time-domain method. Acoustical Science and Technology, 2008;29(4):256–265.

[3] Okuzono T, Otsuru T, Tomiku R, Okamoto N. Fundamental accuracy of time domain finite element method for sound field analysis of rooms. Applied Acoustics. 2010;71(10):940–946.

[4] Okuzono T, Otsuru T, Tomiku R, Okamoto N. Application of modified integration rule to time-domain finite-element acoustics simulation of rooms. The Journal of the Acoustical Society of America. 2012;132(2):804–813.

[5] Mehra R, Raghuvanshi N, Savioja L, Lin MC, Manocha, D. An efficient GPU-based time domain solver for the acoustic wave equation. Applied Acoustics. 2012;73:83–94.

[6] Simonaho SP, Lähivaara T, Huttunen T. Modeling of acoustic wave propagation in time-domain using the discontinuous Galerkin method – A comparison with measurements. Applied Acoustics. 2012;73:173-183.

[7] Okuzono T, Otsuru T, Tomiku R, Okamoto N. A finite-element method using dispersion reduced spline elements for room acoustics simulation. Applied Acoustics. 2014;79:1–8.

[8] Toyoda M, Eto D. Prediction of microperforated panel absorbers using the finite-difference time domain method, Wave Motion. 2019;86:110–124.

[9] Okuzono T, Shimizu N, Sakagami K. Predicting absorption characteristics of single-leaf permeable membrane absorbers using finite element method in a time domain. Applied Acoustics. 2019;151:172–182.

[10] Yue B, Guddati MN. Dispersion-reducing finite elements for transient acoustics. The Journal of the Acoustical Society of America. 2005;118(4):2132–2141.

[11] Sakagami K, Kiama M, Morimoto M, Takahashi D. Detailed analysis of the acoustic properties of a permeable membrane. Applied Acoustics. 1998;54(2):93–111.

[12] Sakagami K, Funahashi K, Somatomo Y, Okuzono T, Nishikawa C, Toyoda M. An experimental study on the absorption characteristics of a three-dimensional permeable membrane space sound absorber. Noise Control Engineering Journal. 2015;63(3):300–307.

[13] Sakagami K, Okuzono T, Somatomo Y, Funahashi K, Toyoda M. A basic study on a rectangular plane space sound absorber using permeable membranes. Sustainability. 2019;11(7):2185.

[14] Ingard KU. Note on Sound Absorption Technology, Noise Control Foundation, New York (USA), 1994.